2001

Control of Phytoplankton Growth by Iron and Silicic Acid Availability in the Subantarctic Ocean: Experimental Results From the SAZ Project

D. A. Hutchins

Peter N. Sedwick
Old Dominion University, Psedwick@odu.edu

G. R. DiTullio

P. W. Boyd

B. Queguiner

See next page for additional authors

Original Publication Citation

Hutchins, D.A., Sedwick, P.N., DiTullio, G.R., Boyd, P.W., Queguiner, B., Griffiths, F.B., & Crossley, C. (2001). Control of phytoplankton growth by iron and silicic acid availability in the subantarctic Southern Ocean: Experimental results from the SAZ project. *Journal of Geophysical Research-Oceans, 106*(C12), 31559-31572. doi: 10.1029/2000JC000333

JOURNAL OF GEOPHYSICAL RESEARCH, VOL. 106, NO. C12, PAGES 31,559-31,572, DECEMBER 15, 2001

Control of phytoplankton growth by iron and silicic acid availability in the subantarctic Southern Ocean: Experimental results from the SAZ Project

D. A. Hutchins,[1] P. N. Sedwick,[2] G. R. DiTullio,[3] P. W. Boyd,[4] B. Quéguiner,[5] F. B. Griffiths, and C. Crossley.

Abstract. Subantarctic Southern Ocean surface waters in the austral summer and autumn are characterized by high concentrations of nitrate and phosphate but low concentrations of dissolved iron (Fe, ~0.05 nM) and silicic acid (Si, <1 μM). During the Subantarctic Zone AU9706 cruise in March 1998 we investigated the relative importance of Fe and Si in controlling phytoplankton growth and species composition at a station within the subantarctic water mass (46.8°S, 142°E) using shipboard bottle incubation experiments. Treatments included unamended controls; 1.9 nM added iron (+Fe); 9 μM added silicic acid (+Si); and 1.9 nM added iron plus 9 μM added silicic acid (+Fe+Si). We followed a detailed set of biological and biogeochemical parameters over 8 days. Fe added alone clearly increased community growth rates and nitrate drawdown and altered algal community composition relative to control treatments. Surprisingly, small, lightly silicified pennate diatoms grew when Fe was added either with or without Si, despite the extremely low ambient silicic acid concentrations. Pigment analyses suggest that lightly silicified chrysophytes (type 4 haptophytes) may have preferentially responded to Si added either with or without Fe. However, for many of the parameters measured the +Fe+Si treatments showed large increases relative to both the +Fe and +Si treatments. Our results suggest that iron is the proximate limiting nutrient for chlorophyll production, photosynthetic efficiency, nitrate drawdown, and diatom growth, but that Si also exerts considerable control over algal growth and species composition. Both nutrients together are needed to elicit a maximum growth response, suggesting that both Fe and Si play important roles in structuring the subantarctic phytoplankton community.

1. Introduction

Some parts of the Southern Ocean such as the Antarctic divergence are thought to be net sources of CO_2 to the atmosphere. Others, such as the Subantarctic Zone (SAZ) north of the Polar Front, are thought to be major CO_2 sinks [*Metzl et al.*, 1999]. The factors that control biological carbon fixation in this region are only partly understood, but limitations due both to insufficient iron supplies and light are undoubtedly important [*Martin and Gordon*, 1990; *Martin et al.*, 1991; *Cullen*, 1991; *Nelson and Smith*, 1991; *Sunda and Huntsman*, 1997; *Boyd et al.*, 1999]. Iron availability exerts a primary control on phytoplankton growth south of the Polar Front, where persistent upwelling delivers high concentrations of nitrate, phosphate, and silicic acid into surface waters [*Martin and Gordon*, 1990; *Martin et al.*, 1991; *de Baar et al.*, 1990, 1995; *Buma et al.*, 1991; *Boyd et al.*, 1999]. Much less is known about the vast subantarctic region north of the Polar Front, although it comprises roughly 50% of the open Southern Ocean [*Boyd et al.*, 1999], supports ~10% of oceanic primary productivity [*Banse*, 1996], and is of global biogeochemical importance [*Kumar et al.*, 1995].

Like the region south of the Polar Front, much of the subantarctic region is likely characterized by low iron concentrations in the upper ocean [*Sedwick et al.*, 1997; 1999] and deep mixed layers due to high wind stress [*Nelson and Smith*, 1991; *Rintoul and Trull*, this issue]. However, the subantarctic surface waters exhibit an important difference from those south of the Polar Front. Although Subantarctic waters are generally replete with nitrate and phosphate, silicic acid is typically depleted to levels near or below measured half-saturation constants for diatom uptake (0.5- 4.6 μM Si) during summer and autumn [*Nelson and Brzezinski*, 1990; *Nelson and Tréguer*, 1992; *Dugdale et al.*, 1995; *Trull et al.*, this issue]. The Subantarctic region is by far the largest "high-nitrate, low-silicic acid" regime in the world ocean, although such conditions also occur in parts of the equatorial Pacific [*Dugdale and Wilkerson*, 1998], and in the coastal upwelling areas off Peru [*Minas and Minas*, 1992] and California [*Hutchins and Bruland*, 1998]. The waters that supply advected nutrients to these regions initially contain high concentrations of nitrate, phosphate, and silicic acid. Thus the preferential depletion of silicic acid relative to nitrate and phosphate in the euphotic zone indicates unbalanced removal processes for this nutrient.

In iron-replete waters, diatoms use silicic acid and nitrate at the "normal" molar ratio of 1:1 [*Brzezinski*, 1985], leading to a

[1]College of Marine Studies, University of Delaware, Lewes, Delaware, USA. (dahutch@udel.edu)
[2] Antarctic CRC, Hobart, Tasmania, Australia.
[3]Grice Marine Laboratory, University of Charleston, Charleston, SC, USA
[4]NIWA Centre for Chemical and Physical Oceanography, University of Otago, Dunedin, New Zealand
[5]Centre d'Océanologie de Marseille, Marseille, France
[6]CSIRO, Division of Marine Research, Hobart, Tasmania, Australia
[7]Institute of Antarctic and Southern Ocean Studies, University of Tasmania, Hobart, Tasmania, Australia

Paper number 2000JC000333.
0148-0227/01/2000JC000333$09.00

relatively balanced drawdown of N and Si. However, reduced iron availability can significantly alter community nutrient utilization ratios, leading to the growth of heavily silicified diatoms, which use silicic acid and nitrate at molar ratios of 2:1 or greater [*Hutchins and Bruland*, 1998; *Takeda*, 1998; *Hutchins et al.*, 1998; *Franck et al.*, 2000]. The biogeochemical consequence is preferential drawdown and export of Si relative to N. Thus community iron deficiency is a likely cause of high-nitrate, low-silicic acid conditions [*Hutchins and Bruland*, 1998], together with the preferential export of Si relative to N by grazers [*Dugdale et al.*, 1995].

In low-iron oceanic regions the eventual depletion of mixed layer silicic acid might lead to a secondary limitation of diatom growth by silicic acid deficiency, thus imposing a major constraint on nitrate drawdown and carbon export. Such low-Fe, low-Si conditions may favor the growth of nonsiliceous, ammonium-driven, iron-efficient phytoplankton species such as eukaryotic picoplankton and cyanobacteria, which indeed commonly dominate the subantarctic autotrophic community [*Wright et al.*, 1996; *Chang and Gall*, 1998]. Of particular interest are the biological and biogeochemical responses of such silicic acid-depleted systems to the addition of iron, such as might accompany short-term atmospheric deposition events or long-term environmental changes.

We conducted shipboard bottle incubation experiments during voyage AU9706 of RSV *Aurora Australis* in the Australian Subantarctic region in March 1998 to understand better the roles of iron and silicic acid in controlling phytoplankton growth rates, community structure, and nutrient cycling in this region. Iron and silicic acid alone and in combination were added to collected seawater, and its resident plankton community within the high-nitrate, low-silicic acid subantarctic water mass. In concurrent shipboard experiments examining the relative importance of light and iron in regulating primary production at this station, *Boyd et al.* [this issue] concluded that iron availability was the primary limitation on autotrophic production within the relatively shallow, transient mixed layer. *Sedwick et al.* [1999] present water column profiles of iron, nutrients and chlorophyll *a*, as well as preliminary results from our Fe and Si addition bottle incubation experiments, which indicate that iron was the proximate limiting nutrient at this station.

Here we present the complete results from these experiments, including analyses of dissolved nutrients, particulate organic carbon and nitrogen, phytoplankton chlorophyll *a* and accessory pigments, algal production and photosynthetic efficiency, phytoplankton cell counts, and iron and silicic acid uptake rates. These results indeed indicate that iron was the proximate limiting nutrient for many biological and biogeochemical processes; however, they also indicate that silicic acid availability exerted a significant control on phytoplankton growth and species composition as well. Our experiments suggest that addition of both iron and silicic acid together is necessary to elicit the greatest biological response by the phytoplankton community.

2. Methods

During voyage AU9706 of RSV *Aurora Australis* in March 1998 we collected seawater using a trace metal clean Teflon diaphragm pump [*Hutchins et al.*, 1998] from ~20 m water depth at 46°46'S, 142°E [*Trull et al.*, this issue, Figure 1, process station 2] for shipboard bottle incubation experiments. The seawater was discharged under Class-100 filtered air, where it was gently mixed in acid-cleaned 50 L polyethylene carboys and immediately transferred into the clean, rinsed incubation containers (acid-cleaned 2.4 L Nalgene polycarbonate bottles and 24 L Nalgene polycarbonate carboys). Subsamples for initial (t = 0) analyses (detailed below) were taken directly from the 50 L mixing carboys.

The incubation containers were either (1) enriched with silicic acid (+Si, ~9 μM), (2) enriched with iron (+Fe, 1.9 nM), (3) enriched with iron and silicic acid (+Fe+Si, 1.9 nM and ~9 μM, respectively), or (4) left untreated as controls. Silicic acid additions were calculated to yield final concentrations approximately equal to the ambient nitrate concentrations (~9 μM). Iron was added as a solution of ferric chloride in 0.01 M hydrochloric acid, and silicic acid was added as a solution of trace metal clean sodium metasilicate (purified using chelex-100 ion exchange resin). The silicic acid stock had partially polymerized in the cold conditions of the field laboratory, which resulted in measured dissolved Si concentrations about 20% lower than the nominal initial target concentration. However, our nutrient measurements (see section 3) indicate that the added Si depolymerized in the incubation bottles during the course of the experiment, and we assume that the total concentration of added Si, as dissolved and colloidal silicic acid, was close to the target concentration of 9 μM.

The bottles were sealed and set in circulating surface seawater inside polyethylene deck incubators at ~50% of incident irradiance and were maintained near ambient sea surface temperature (11 ± 2°C) throughout the experiment. For each experimental treatment, duplicate 2.4 L bottles were sacrificed on days 2, 5, and 8 for analyses requiring small sample volumes (dissolved nutrients, size-fractionated chlorophyll *a*, flow cytometry, photosynthesis versus irradiance, etc., detailed below). In addition, for each experimental treatment one 24 L carboy was sacrificed on day 5 for analyses requiring larger sample volumes and to allow us to evaluate any significant container size effects [*Berg et al.*, 1999]. Analyses performed on samples from the 24 L carboys included Fe concentrations, ^{55}Fe uptake rates, phytoplankton accessory pigments, and ^{14}C pigment labeling, in addition to most of the same measurements carried out on the 2.4 L bottles.

Dissolved Fe was measured in the starting seawater (t = 0) and at day 5 in the 24 L carboys only, because of sample volume requirements. Acidified 0.4 μm-filtered samples were analyzed on shore by flow injection analysis using a modification of the method of *Measures et al.* [1995], as detailed by *Sedwick et al.* [1997; 1999]. Dissolved macronutrients (nitrate + nitrite, phosphate and silicic acid) were measured in all incubation containers using syringe-filtered samples (0.45 μm Acrodisc polysulfone) and were determined using a shipboard Alpkem segmented flow analysis system

Size-fractionated chlorophyll *a* (chl *a*, 0.2, 2.0, 5.0, and 20 μM) was determined in all incubation samples as was done by *Boyd et al.* [this issue]. Algal photosynthetic efficiency was measured in the 2.4 L bottles using a Chelsea Instruments Fastracka fast repetition rate fluorometer [*Kolber and Falkowski*, 1993], as described by *Boyd et al.* [this issue]. Primary production and algal photosynthetic parameters were estimated using a small-bottle ^{14}C technique [*Mackey et al.*, 1995], as described by *Boyd et al.* [this issue]. Estimates of the maximum rate of production (P_{max}, mg C m^{-3} h^{-1}) and the initial slope of the light-limited section of the P versus I curve (α, mg C m^{-3} h^{-1} (μmol photons m^{-2} s^{-1})$^{-1}$) were obtained for all treatments in replicate except for the +Fe treatments, for which only one incubation bottle was sampled because of space limitations of the ^{14}C incubation system. Fluorometrically determined chl *a* was used to obtain chl *a* normalized values of P_{max} (P_m^B, mg C (mg chl *a*)$^{-1}$ h^{-1}) and alpha (α^B, mg C (mg chl *a*)$^{-1}$ h^{-1} (μmol photons m^{-2} s^{-1})$^{-1}$).

Three independent methods were used to monitor phytoplankton community composition in the incubation bottles:

phytoplankton accessory pigment analysis, flow cytometry, and visual cell counts by microscopy. Taxon-specific phytoplankton accessory pigments were measured using high-performance liquid chromatography (HPLC). Because of the large sample volume required (1- 3 L), pigments were measured only in the starting seawater (t = 0) and the day 5 subsamples from the 24 L carboys. Samples were filtered (Whatman GF/F) and frozen in liquid nitrogen until analysis as described by *DiTullio et al.* [this issue] and *Hutchins et al.* [1998]. Pigment concentration data were analyzed using the CHEMTAX program [*Wright et al.*, 1996] to estimate the relative abundances of specific taxonomic groups of algae. Taxon-specific phytoplankton intrinsic growth rates were measured on day 5 in the carboys using ^{14}C pigment labeling, as described by *DiTullio et al.* [this issue].

Flow cytometry samples were analyzed live at sea within 1 hour of sampling using a Becton Dickinson FACScan flow cytometer (15 mW argon ion laser, 488 nm excitation) with Lysis II software. Flow rate and size calibration were determined using "Fluoresbrite" beads (Polysciences), and laboratory cultures (e.g. *Synechococcus*, *Pyramimonas*). Phytoplankton were characterized and enumerated using red (chlorophyll, 660-700nm) and orange (phycoerythrin, 530-630 nm) fluorescence [*Olson et al.*, 1993; *Hofstraat et al.*, 1994]. Regional analysis of two-dimensional scatterplots enumerated large, strongly red autofluorescent phytoplankton (e.g., diatoms); smaller red autofluorescent nanoplankton (e.g. prasinophytes and chlorophytes); picophytoplankton with dim red autofluorescence (1-2 μm diameter coccoid cells, largely eukaryotic flagellates); and orange autofluorescent picophytoplankton (e.g., cyanobacteria) [*Durand and Olson*, 1996; *Crossley*, 1998; *Wright et al.*, 1998].

Visual cell counts were carried out on samples from days 2, 5, and 8 in the 2.4 L bottles using 50 mL glutaraldehyde-preserved samples [*Hutchins et al.*, 1998]. Only large cells (pennate and centric diatoms and autofluorescent dinoflagellates) were counted, because of imperfect preservation and dim fluorescence of small taxa. Cell counts in the starting seawater (t = 0) were too low to obtain reliable counting statistics and are not presented. Values for each bottle were calculated as the average of six counts, and values and errors for each treatment are the means and ranges for both duplicate bottles.

Particulate organic carbon (POC) and particulate organic nitrogen (PON) were measured in all incubations as described by *Hutchins et al.* [1998]. Particulate biogenic silica (BSi) and ^{32}Si silica production rate analyses were also performed on all incubation samples, as described by *Quéguiner* [this issue]. Size-fractionated biological Fe uptake was measured in the starting seawater (t = 0) and at day 5 in the 24 L carboys. Duplicate 500 mL subsamples were incubated with 1 nM ^{55}Fe for 6 daylight hours in the deckboard incubators, then filtered (0.2 and 5 μm polycarbonate) with Ti washing to remove surface-bound isotope [*Hudson and Morel*, 1989]. ^{55}Fe was counted using liquid scintillation, and molar Fe uptake rates were calculated using the known specific activity of the isotope and the ambient nonradioactive Fe concentrations [*Schmidt and Hutchins*, 1999]. Iron uptake rates are the means and ranges of duplicate subsamples from each carboy.

3. Results

3.1. Dissolved Iron and Nutrients

The physical and chemical characteristics of the upper water column at this station are presented by *Sedwick et al.* [1999]. This station had a shallow surface mixed layer (20-50 m) that was likely the result of temporary high insolation and low wind conditions [*Boyd et al.*, this issue]. There was a well-developed pycnocline at 80-100 m depth, and the 1% light level was at 84 m depth. Dissolved Fe concentrations throughout the upper water column were 0.11 nM or less and were 0.05 nM at ~20 m depth, where the water was collected for the incubations (Figure. 1a). Nitrate and silicic acid exhibited classic nutrient-type profiles, each with a distinct nutricline between 100 and 130 m depth (Figure. 1b). However, silicic acid concentrations were much lower (0.66-0.80 μM) than nitrate concentrations (9-9.5 μM) throughout the upper water column. Phosphate concentrations ranged from 0.70 μM at 15 m depth to 1.06 μM at 250 m depth (data not shown). The dissolved N:P ratio was 12.9 near the surface and 14.2 at depth, and dissolved Si:P ratios were ~1 to 3.7 over the same depth range. These calculations suggest that P availability was not limiting phytoplankton growth rates relative to N and Si throughout the upper water column.

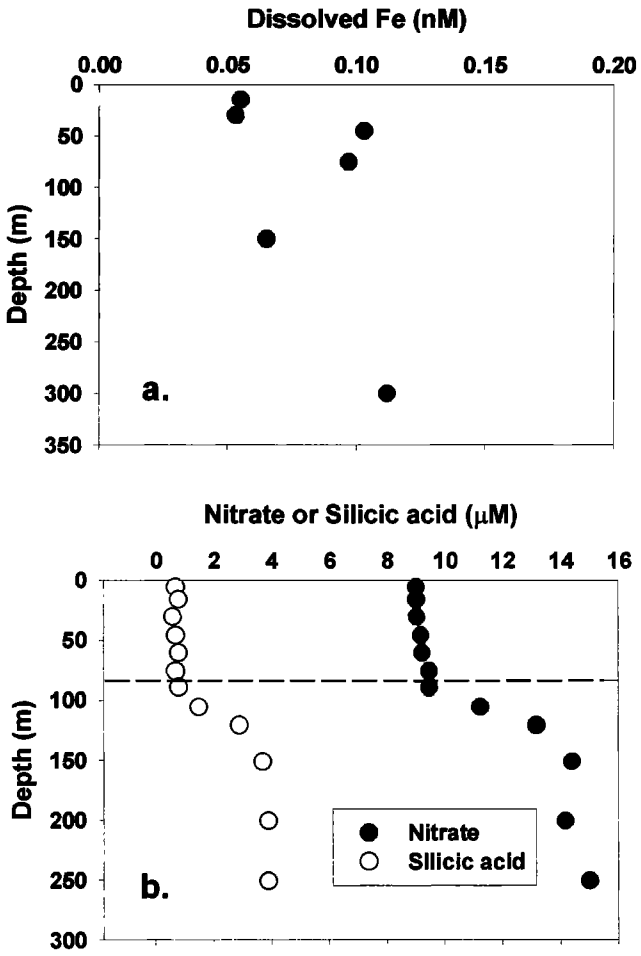

Figure 1. Vertical profiles of dissolved Fe and major nutrients at the station (46.8°S,142.1°E) where water was collected for the incubation experiments: (a) Total dissolved Fe (<0.4 μm) measured by flow injection analysis and (b) Nitrate (solid circles), and silicic acid (open circles). The dashed line denotes the bottom of the euphotic zone (1% light level). Adapted from Sedwick et al., [1999].

3.2. Biological Response

The initial total chl *a* concentration (>0.2 μm) in the water collected for the experiments was low (0.21 μg L^{-1}), and there was little accumulation in any of the 2.4 L bottles

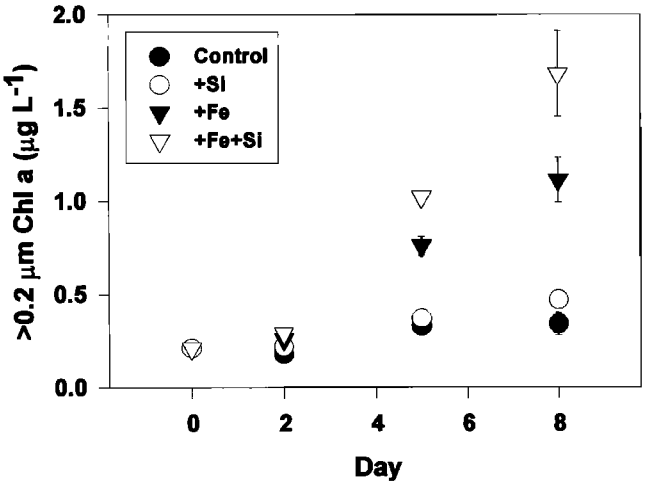

Figure 2. Total chlorophyll *a* (chl *a*, >0.2 µm) in all four treatments over the 8 day incubation. Treatments include unamended controls (solid circles); +9 µM Si (+Si, open circles); + 1.9 nM Fe (+Fe, solid triangles); and + 1.9 nM Fe, +9 µM Si (+Fe+Si, open triangles). Symbols and error bars are the means and ranges of duplicate 2.4 L bottles, respectively. Adapted from *Sedwick et al.*, [1999].

until after the first 2 days of the incubations (Figure 2). Following this apparent lag period, dramatic increases in chl *a* biomass were observed in the +Fe and +Fe+Si treatments, but little increase was evident in either the control treatments or +Si bottles (Figure 2). Chl *a* accumulation was greater in the +Fe+Si bottles than in the +Fe treatments, but as noted by *Sedwick et al.* [1999], this difference was not statistically significant at the 95% confidence level ($p > 0.1$, unpaired Student's *t*- test).

The size-fractionated chl *a* data demonstrate that the response to the added Fe and Si was size class-specific (Figure 3). Initially, most of the chl *a* was present in the smallest size classes. Chl *a* concentrations in the initially-dominant picoplankton size class (0.2-2.0 µm) increased significantly ($p = 0.04$) after addition of Fe and Si together but showed much less response to either nutrient added alone (Figure 3a). In contrast, the increases in chl *a* accumulation in the 2.0- 5.0 µm size class stimulated by +Fe and +Fe+Si additions were statistically insignificant compared to control and +Si treatments (Figure 3b). There were also no statistically significant differences between chl *a* concentrations in the 5.0- 20 µm size class in all four treatments ($p > 0.09$, Figure 3c). The largest size class (>20 µm) apparently benefited from the added Fe, as chl *a* concentrations in the +Fe+Si treatments were significantly higher ($p < 0.04$) than those in the control and +Si treatments by the end of the incubation (Figure 3d). Chl *a* was also higher in this largest size class in the +Fe bottles compared to the control and +Si treatments, although this difference was not statistically significant ($p > 0.09$). Differences in final chl *a* concentrations in the >20 µm size class between the +Fe+Si and +Fe treatments were also not significant ($p = 0.09$).

Net chl *a*-specific growth rates (d^{-1}) in the 2.4 L bottles between day 2 (at the end of the initial "lag period") and day 8 are presented in Table 1. For both the whole phytoplankton community (> 0.2 µm) and for each size class, +Fe+Si additions resulted in the highest net growth rates. These increases were only minor in the picoplankton size class (0.2- 2.0 µm), relative to the +Fe and +Si treatments, but were striking in the larger size classes. Compared to the control treatments, net chl *a*-specific growth rates in the +Fe+Si bottles were 3.5 times greater in the >20 µm size class, 3.6 times greater in the 5.0- 20 µm size class, and 2.3 times greater in the 2.0- 5.0 µm size class. Addition of Fe alone resulted in smaller increases in net chl *a*-specific growth

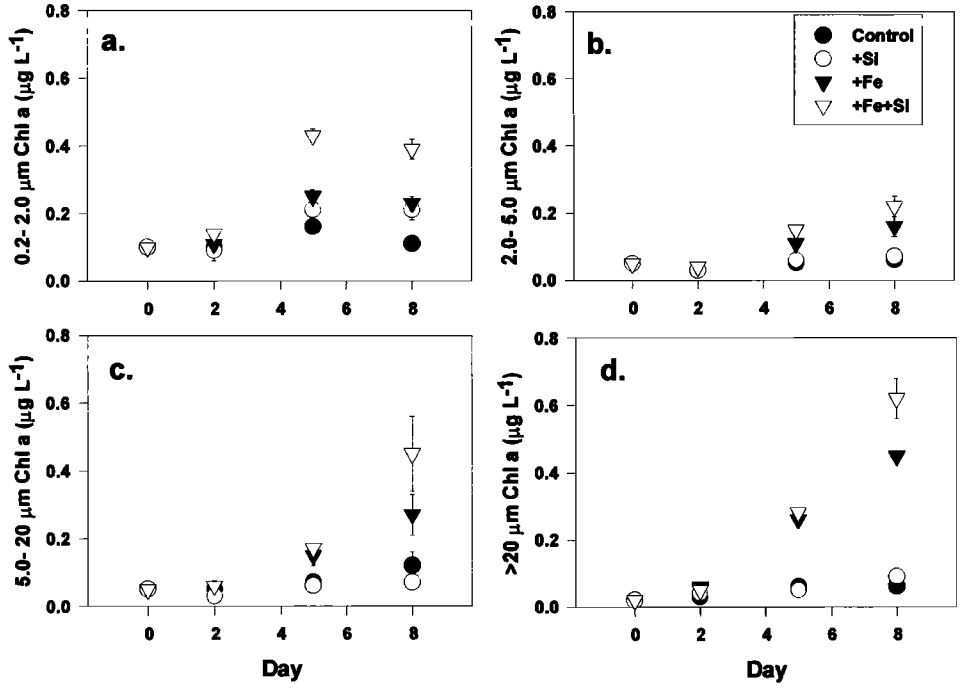

Figure 3. Size-fractionated chl *a* in all four incubation treatments, including: (a) the 0.2-2 µm size class, (b) the 2- 5 µm size class, (c) the 5-20 µm size class, and (d) the >20 µm size class. Symbols and error bars are as in Figure 2.

Table 1. Chlorophyll *a* net specific growth rates in each treatment between days 2 and 8 of the incubations for the whole phytoplankton community (>0.2 μm) and four phytoplankton size classes.

Treatment	>0.2 μm	0.2- 2.0 μm	2.0- 5.0 μm	5.0- 20 μm	>20 μm
Control	0.09	0.02	0.12	0.15	0.12
+Fe	0.24	0.12	0.23	0.25	0.34
+Si	0.13	0.14	0.14	0.09	0.14
+Fe+Si	0.29	0.17	0.28	0.34	0.42

rates compared to the control treatments. Addition of Si alone had little or no effect on all size classes except for the picoplankton fraction (0.2- 2.0 μm, Table 1), which had much higher net chl *a* growth rates after Si addition.

The net chl *a* specific growth rates between days 2 and 8 were low compared to intrinsic growth rates as estimated by ^{14}C pigment labeling on day 5. Chlorophyll labeling indicates that intrinsic growth rates were highest on day 5 in the +Fe+Si and +Fe treatments (1.39 and 0.96 d^{-1}, respectively) and lowest in the control and +Si treatments (0.45 and 0.34 d^{-1}, respectively). Net growth rates are underestimates of the true cellular growth rate, because of grazing losses.

Phytoplankton photosynthetic efficiency measurements in the 2.4 L incubation bottles using fast repetition rate fluorometry are presented in Figure 4. Initial F_v/F_m values in the starting seawater (t = 0) were about 0.25, suggesting impaired photosystem functioning [*Kolber and Falkowski*, 1993]. By the second day of the incubations, F_v/F_m in the +Fe and +Fe+Si bottles had increased significantly relative to the control and +Si treatments (p = 0.02) and remained significantly elevated relative to the control and Si treatments until the end of the experiment (p< 0.04). These Fe-induced increases in F_v/F_m were similar to those observed in open ocean and bottle Fe addition experiments carried out south of the Polar Front [*Boyd et al.*, 2000; *Olsen et al.*, 2000]. The F_v/F_m ratios in the control and Si treated bottles were similar, although slightly higher in the +Si-treatments on day 5. Si addition alone did not result in significant increases in F_v/F_m (Figure 4) however, contrary to the results of a recent study using laboratory diatom cultures [*Lippemeier et al.*, 1999]. The F_v/F_m ratios declined in all treatments between days 2 and 8, perhaps due to an increase or onset in Fe deficiency in the bottles as biomass increased. Even the highest F_v/F_m ratios measured in the +Fe and +Fe+Si treatments were below values measured in surface waters in the SAZ during the cruise (0.4-0.45), and those typical of nutrient-replete phytoplankton in the laboratory (~0.6) [*Greene et al.*, 1991; *Kolber and Falkowski*, 1993]. Lower F_v/F_m values in our study could reflect stress due to low levels of Si or thermal stress during sample handling and analysis.

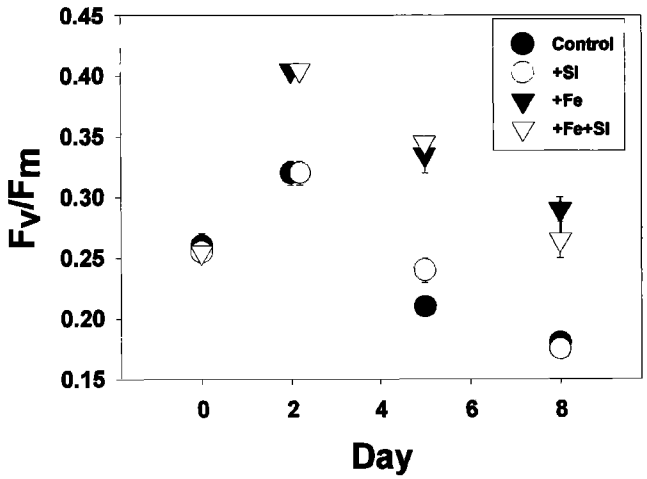

Figure 4. Variable over maximum fluorescence yield of photosynthesis (F_v/F_m) as measured by fast repetition rate fluorometry during the 2.4 L bottle incubations, a measure of phytoplankton photosynthetic efficiency. Symbols and error bars are as in Figure 2.

Final photosynthetic carbon fixation rates from the P versus I measurements at saturating light intensity (P_{max}) in +Fe bottles were more than twice as high as those in +Si or control treatment bottles, but final P_{max} values for the +Fe+Si treatments were more than twice as high again as those in the +Fe bottles (Figure 5a). However, when these values are corrected for Fe-induced increases in phytoplankton chl *a*, P_m^B rates in +Fe+Si- and +Fe-treated bottles were only slightly higher than those in the control and +Si treatments, with the exception of a single high value measured in the +Fe bottles on day 5 (Figure 5b). These observations suggest that increases in chl *a*-specific phytoplankton photosynthetic efficiency with the addition of iron were not large, consistent with the F_v/F_m data. The final values of alpha (α) were also much higher in the +Fe+Si treatments relative to the other three treatments, and +Fe treatment values were slightly elevated relative to the +Si and control treatment bottles (Figure 5c). Again, however, these differences disappear when values are normalized to chl *a* (α^B, Figure 5d). This may suggest no real increase in chl *a*-normalized photosynthetic C fixation efficiency after Fe addition, but Fe addition usually results in much higher chl *a* $cell^{-1}$ [*Geider and LaRoche*, 1994]. For instance, chl *a* $cell^{-1}$ nearly doubled in Fe-amended treatments from the Fe/light limitation experiment we carried out at this station [*Boyd et al.*, this issue]. Thus carbon fixation per cell could still have increased substantially, but this may not have been evident from normalization of photosynthetic parameters to bulk chl *a* concentrations.

HPLC measurements of photosynthetic accessory pigments suggest that both diatoms and haptophytes dominated growth in the carboys treated with Fe and/or Si (Figure 6). Concentrations of fucoxanthin, generally characteristic of diatoms [*Jeffrey et al.*, 1997] increased dramatically in the +Fe+Si-treated carboy relative to the initial (11 times) and day 5 control (4.4 times) values and also increased to a slightly lesser extent in the +Fe- and +Si-treated carboys (Figure 6). A similar pattern was observed for 19-hexanoyloxyfucoxanthin (19-hex, characteristic of haptophytes), alloxanthin (cryptophytes), and 19-butanoyloxyfucoxanthin (19-but, pelagophytes) [*Jeffrey et al.*, 1997], which also increased in +Fe- , +Si-, and +Fe+Si-treated bottles relative to the control bottles. Peridinin, diagnostic of dinoflagellates [*Jeffrey et al.*, 1997], was initially present in low concentrations and did not change markedly in the various treatments. Differences in the concentrations of lutein (chlorophytes), chlorophyll *b* (chlorophytes, prasinophytes, and prochlorophytes), and zeaxanthin (prochlorophytes and *Synechococcus*) [*Jeffrey et al.*, 1997] were quite small among treatments, suggesting that net growth of these groups was negligibly affected by Fe or Si addition. Substantial increases in phaeophorbides in all but the control bottles (Figure 6) suggest enhanced grazing with Fe and Si addition, particularly in the +Fe+Si treatment.

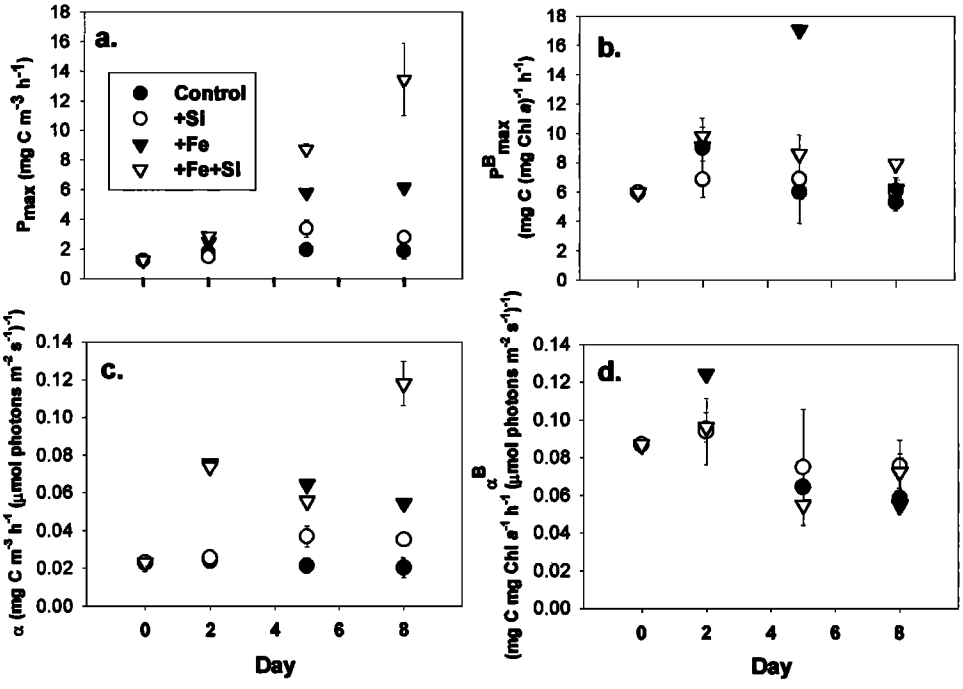

Figure 5. Photosynthesis versus irradiance (P versus I) parameters in the four treatments during the 2.4 L bottle incubations: (a) P_{max}, the maximum (light-saturated) carbon fixation rate normalized on a volume basis, (b) P_m^B, normalized to chl *a* concentrations in the treatments, (c) α, the slope of the initial (light-limited) portion of the P versus I curve normalized on a volume basis, and (d) α^B, normalized to chl *a* concentrations in the treatments. Symbols and error bars are as in Figure 2, except that +Fe samples are from measurements of a single bottle rather than duplicates (see section 2) and therefore do not include error bars.

Results of the CHEMTAX analyses of the phytoplankton pigment data are presented in Table 2. These calculations suggest that diatoms accounted for only about 10% of the total community photosynthetic pigments on day 0. This percentage increased about 2 times in the control and +Si carboys by day 5 but increased much more (~3 times) in the +Fe and +Fe+Si treatments. CHEMTAX results suggest that the initial assemblage was dominated by chlorophytes (41% of total pigments) but this group declined in all treatments about equally to final values of 24- 27% by day 5. Type 3 haptophytes (including coccolithophorids and some species of *Phaeocystis*) were also initially prominent (16% of total pigments) but declined dramatically in all treatments except the control by day 5. Type 4 haptophytes (including chrysophytes such as silicoflagellates, pelagophytes, and parmales and some *Phaeocystis* species such as *Phaeocystis antarctica*) were initially also abundant (21% of total pigments) but increased only slightly in the control and +Fe treatments. These type 4 haptophytes did increase significantly by day 5 (~34% of total pigments) in both treatments with Si added, however, perhaps reflecting the growth of silicoflagellates or silicified parmales in response to the Si additions. Of the minor algal taxa present at the initial timepoint, CHEMTAX suggested that dinoflagellates, prasinophytes, and all cyanobacteria (including *Synechococcus* and *Prochlorococcus*) declined in all treatments by day 5 (Table 2). *Synechococcus* was the dominant cyanobacterium in our samples, as *Prochlorococcus* pigments were very scarce (initial) or absent (final, all treatments, Table 2). Of the initially rare taxa, only cryptophytes increased in relative abundance in the experimental carboys, especially those with Fe and/or Si added. *Olsen et al.* [2000] found that cryptophytes were the only algal group that did not respond to Fe additions in other Southern Ocean waters.

Flow cytometric estimates of all red fluorescent nanoplankton are assumed to represent eukaryotic phytoplankton since prochlorophytes were rare or absent in our samples (see above). Red fluorescent nanoplankton increased significantly ($p < 0.05$) in the +Fe+Si treatment relative to all three of the other treatments and in the +Si and +Fe treatments relative to the controls (Figure 7a). Very strongly red fluorescent nanoplankton, thought to be mostly diatoms, increased dramatically in the Fe-amended bottles (+Fe and +Fe+Si) compared to the low levels in the control and +Si treatments ($p < 0.04$, Figure 7b). Dimly red fluorescent picoplankton that likely represent small eukaryotic flagellates increased significantly in the Si-treated bottles (+Si and +Fe+Si, Figure 7c), supporting the results of the CHEMTAX pigment analyses showing increases in Type 4 haptophytes in these treatments (Table 2). Orange fluorescing picoplankton representing cyanobacteria (Figure 7d) increased in all bottles by day 2, followed by losses to final values close to or less than initial values on day 8, and there were no significant differences between treatments.

Microscopic cell counts of large phytoplankton taxa are presented in Table 3. It should be noted that some difference is expected from the flow cytometry data, which are biased toward the counting of small particles and unable to distinguish algal species (or indeed algal cells from other fluorescent particles). Nanoplanktonic pennate diatoms (<5 μm) were abundant in the incubation samples, mostly belonging to the genera *Nitzschia*,

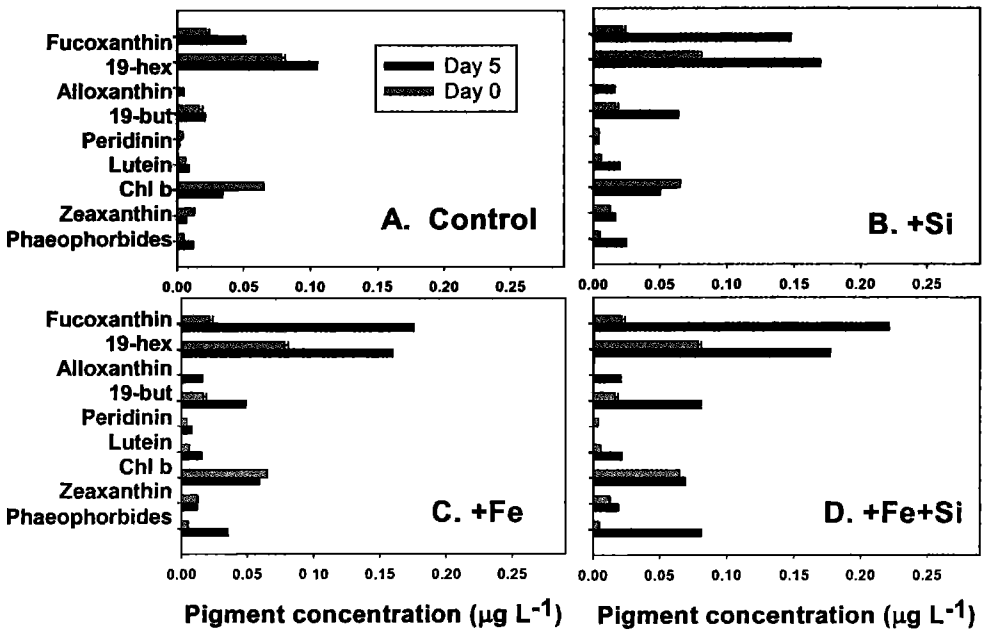

Figure 6. Phytoplankton taxon-specific photosynthetic pigment concentrations in the initial collected water samples (shaded bars) and on day 5 of the incubations (black bars) in the 24 L carboys: (a) controls, (b) +9 μM Si (+Si), (c) +1.9 nM Fe (+Fe), and (d) +1.9 nM Fe and +9 μM Si (+Fe+Si). Values and error bars of the initial samples are the means and ranges of duplicate samples; day 5 values are single samples only. Pigments measured include fucoxanthin (diatoms), 19-hex (haptophytes), alloxanthin (cryptophytes), 19-but (pelagophytes), peridinin (dinoflagellates), lutein (chlorophytes), chl *b* (chlorophytes and prochlorophytes), zeaxanthin (cyanobacteria including *Synechococcus* and prochlorophytes), and combined phaeophorbides (produced by degradation of chl *a* by grazing in the bottles).

Pseudo-nitzschia, *Cylindrotheca*, and *Navicula*. The abundance of small pennate diatoms increased in all treatments, but final cell numbers were significantly higher in the +Fe- and +Fe+Si-treated bottles (~10,000 cells mL^{-1}, $p < 0.05$) than in the +Si and control treatments (~1400-2250 cells mL^{-1}). This is also suggested by the strongly red fluorescent cell increases measured by flow cytometry in Fe-amended bottles (Figure 7b). Centric diatoms (including Coscinodiscaceae and the genus *Chaetoceros*, among others) were not abundant (163 - 950 mL^{-1}), and there were no significant differences among treatments, except for lower numbers in the +Si bottles. Autofluorescent dinoflagellates were present in similar numbers in the control, +Fe and +Fe+Si treatments on day 8 (~1000- 1300 mL^{-1}), but like centric diatoms, were significantly less abundant in the +Si bottles (~500 mL^{-1}).

3.3. Nutrient Biogeochemistry

Consistent with the results of previous shipboard Fe- addition experiments in other low-iron oceanic regimes, considerably more nitrate was consumed in 2.4 L bottles treated with Fe (+Fe: 4.1 μM, +Fe+Si: 5.4 μM) than in the control treatments (1.1 μM), and only slightly more nitrate was consumed in the +Si treatments (1.7 μM) relative to the control samples (Figure 8a). Final nitrate concentrations were significantly ($p < 0.002$) lower in both

Table 2. Results of CHEMTAX analyses (*Wright et al.*, 1996) of phytoplankton accessory pigment concentrations in the initial collected water and on day 5 in the 24-L carboys.

Phytoplankton Group		Day 5			
	Initial	Control	+Si	+Fe	+Fe+Si
Diatoms	10.2 ± 0.8	22.1	23.7	32.8	29.2
Chlorophytes	41.1 ± 1.5	27.9	27.5	24.9	24.3
Haptophytes 3	16.4 ± 1.1	18.2	2.3	6.6	0
Haptophytes 4	20.8 ± 2.5	23.1	33.6	24.5	34.4
Dinoflagellates	1.6 ± 0.2	0.8	0.6	1.4	0
Prasinophytes	1.4 ± 0.1	0	0	0	0
Cryptophytes	0.1 ± 0	4.4	7.5	7.0	7.7
Cyanobacteria	8.3 ± 0.6	3.4	4.8	2.8	4.3
Prochlorococcus	0.2 ± 0	0	0	0	0

[a]CHEMTAX analyses are discussed by *Wright et al.*, [1996]. Results are presented as the percentage of total phytoplankton pigments found in each algal taxonomic group. Initial values are the means and ranges of duplicate measurements; day 5 values are from single carboys.

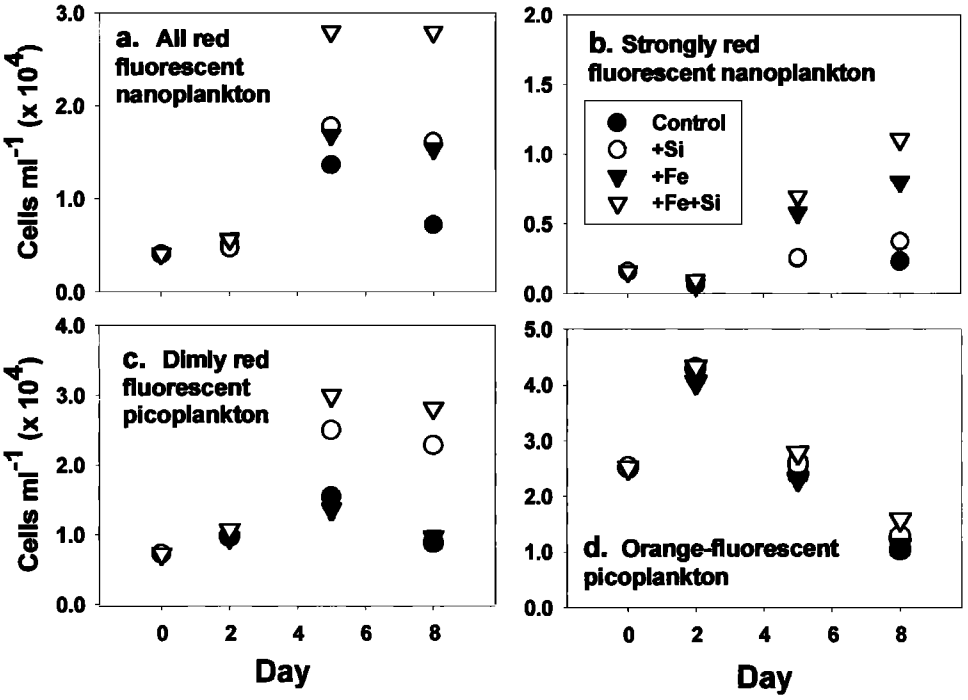

Figure 7. Flow cytometric measurements of phytoplankton groups in all four treatments in the 2.4 L bottle incubations, including: (a) all red fluorescent nanoplankton cells, (b) strongly red fluorescent nanoplankton, mostly diatoms, (c) dimly red fluorescing cells, including eukaryotic picoplankton, and (d) orange fluorescent cells only, comprised of cyanobacteria, mostly *Synechococcus*. Symbols are as in Figure 2.

treatments with added Fe compared to the control and +Si treatments. Trends in phosphate utilization were very similar (Figure. 8b), with amounts consumed ranging from 0.07 μM (controls) to 0.33 μM (+Fe+Si). As for nitrate, final phosphate concentrations were significantly lower in +Fe and +Fe+Si bottles ($p < 0.03$) relative to the control and +Si treatments.

Even with the large addition of silicic acid to the +Si and +Fe+Si bottles (~9 μM, relative to the ambient concentration of 0.66 μM), consumption of this nutrient was much less than was observed for nitrate (Figure 8c). Partial polymerization of the added silicic acid stock solution (see section 2) prevents an accurate evaluation of Si consumption in the +Si- and +Fe+Si-treated bottles. The small increases in measured dissolved silicic acid concentrations in these bottles between days 2 and 5 are thought to reflect depolymerization of the added Si stock. Overall, the +Si-treated bottles apparently consumed only ~0.5 μM silicic acid, while a 3-4 times greater drawdown was observed in the +Fe+Si treated bottles (~2 μM Si consumed), although this difference was not statistically significant (p = 0.07). In the control and +Fe treatment bottles, silicic acid concentrations remained low (Figure 8c), with 0.15 (control) and 0.57 μM (+Fe) dissolved Si consumed over the course of the 8 day incubations.

Silicic acid to nitrate (Si:N) molar drawdown (i.e., net consumption) ratios were quite low in all of the treatments, ranging from 0.13 to 0.35, and showed no apparent dependence on the addition of Fe to incubated samples. These molar drawdown ratios are much lower than the Si:N uptake ratio of unity that is typical of most species of diatoms grown under nutrient-replete conditions [*Brzezinski*, 1985], even allowing for the uncertainty in Si drawdown in the +Si and +Fe+Si treatments due to polymerization of the added Si stock solution. The molar ratios of net Si:N drawdown were 0.13 (control), ~0.32 (+Si), 0.14 (+Fe), and ~0.35 (+Fe+Si) and do not exhibit the trend,

Table 3. Microscopic cell counts (cells ml^{-1}) of pennate and centric diatoms and autofluorescent dinoflagellates in all four treatments in the 2.4-L bottles on days 2, 5 and 8 of the incubations. Initial (Day 0) cell numbers of these large cells were too low for good counting statistics. Values and errors are the means and ranges of counts from duplicate bottles.

Treatment	Pennate diatoms			Centric diatoms			Dinoflagellates		
	Day 2	Day 5	Day 8	Day 2	Day 5	Day 8	Day 2	Day 5	Day 8
Control	365 (±320)	598 (± 177)	2251 (± 1591)	80 (± 80)	211 (± 114)	482 (± 180)	558 (± 0.4)	711 (± 130)	1277 (± 45)
+Fe	38 (±38)	2019 (± 281)	9489 (± 1497)	258 (± 118)	1382 (± 301)	950 (± 643)	560 (± 10)	856 (± 177)	1023 (± 302)
+Si	128 (± 53)	2935 (± 339)	1392 (± 202)	40 (± 40)	365 (± 285)	163 (± 138)	641 (± 20)	827 (± 86)	497 (± 165)
+Fe+Si	313 (± 169)	3625 (± 1368)	10071 (± 495)	489 (± 338)	None observed	693 (± 196)	572 (± 74)	1205 (± 132)	1293 (± 721)

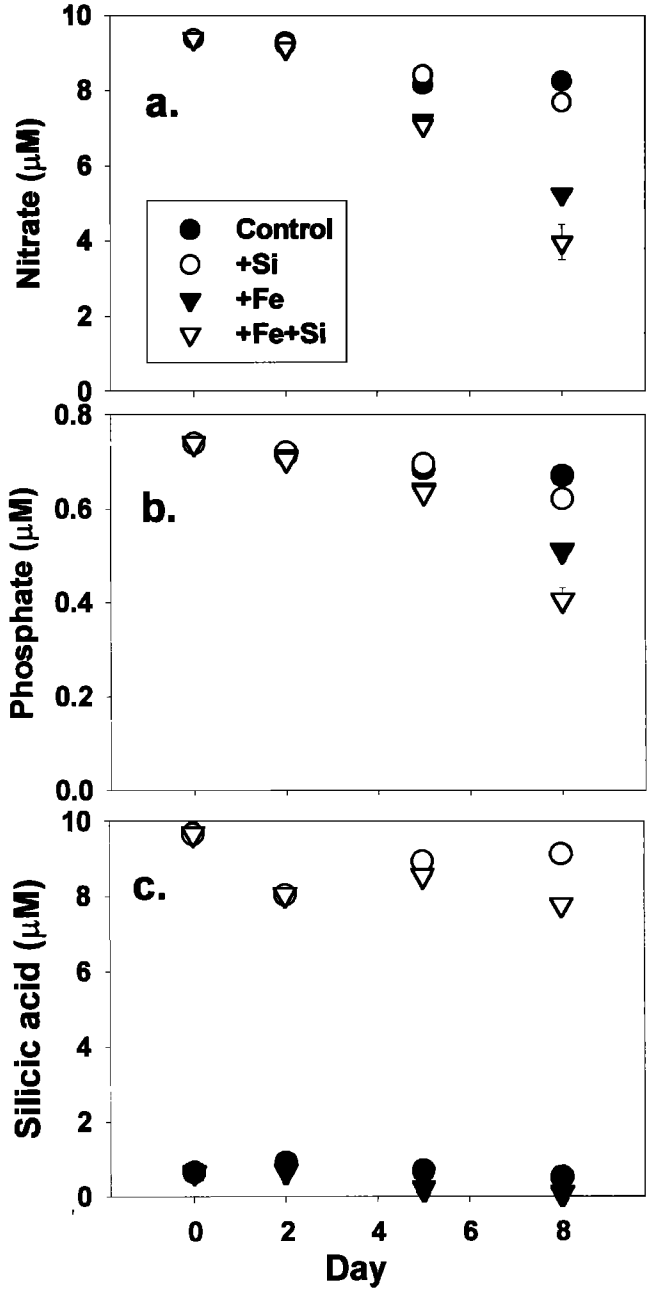

Figure 8. (a) Nitrate, (b) phosphate, and (c) silicic acid concentrations in all four treatments over the course of the 2.4 L bottle incubations. Symbols and error bars are as in Figure 2.

which has been observed in other low-Fe oceanic regimes, in which Si:N community drawdown ratios range from 2 to 3 under Fe-deficient conditions to near unity in bottles treated with Fe [*Hutchins and Bruland*, 1998; *Takeda*, 1998, *Boyd et al.*, 2000].

The concentrations of PON in the starting seawater (t = 0) were low (0.42 μmol L^{-1}) but increased in all treatments in the 2.4 L bottles over the incubation period (Figure 9a). The controls produced only 1.8 μmol L^{-1} PON over 8 days, similar to the increases of 2.1 μmol L^{-1} in the +Si treatment bottles and only slightly less than the 2.6 μmol L^{-1} produced in the +Fe treatment bottles. Differences among these three treatments were not significant at the $p < 0.05$ confidence level. Although 4.1 μmol L^{-1} PON was produced in the +Fe+Si treatment, this increase was not statistically different (p = 0.09) from the PON increases measured in the other treatments (Figure. 9a). Mass balance calculations indicate that molar amounts of N produced as PON comprised 161% (controls), 121% (+Si), 63% (+Fe), and 75% (+Fe+Si) of the total amount of nitrate consumed (Figure. 9a). This suggests that alternate nonnitrate sources of nitrogen (such as ammonium) were converted into PON in the treatments without added Fe [*Price et al.*, 1991], as well as possible losses of assimilated nitrate as ammonium and/or dissolved organic nitrogen [*Bronk and Ward*, 1999] in the +Fe and +Fe+Si bottles.

POC concentration was also low in the starting seawater (t = 0) at 4.6 μmol L^{-1} (Figure 9b). During the course of the incubations, POC production followed a similar pattern to PON production, with the following concentrations produced: 16.7 μmol L^{-1} (+Si), 24.7 μmol L^{-1} (controls), 28.8 μmol L^{-1} (+Fe), and 35.9 μmol L^{-1} (+Fe+Si). As with the PON and chl a results, the final POC concentrations were highest in +Fe+Si treated bottles (Figure 9b), although differences in POC produced among the different treatments were not statistically significant (p = 0.08) at the level of replication used in this experiment.

BSi concentrations in the 2.4 L bottles increased slightly in the control treatments during the incubations; however, there were significantly greater increases in the other treatments (Figure 10a). Relative to control samples, BSi concentrations were 1.8 times higher in the +Si treatments, and 2.4 times higher in the +Fe treatments. The greatest increases were observed in the +Fe+Si-treated bottles, in which final BSi concentrations were

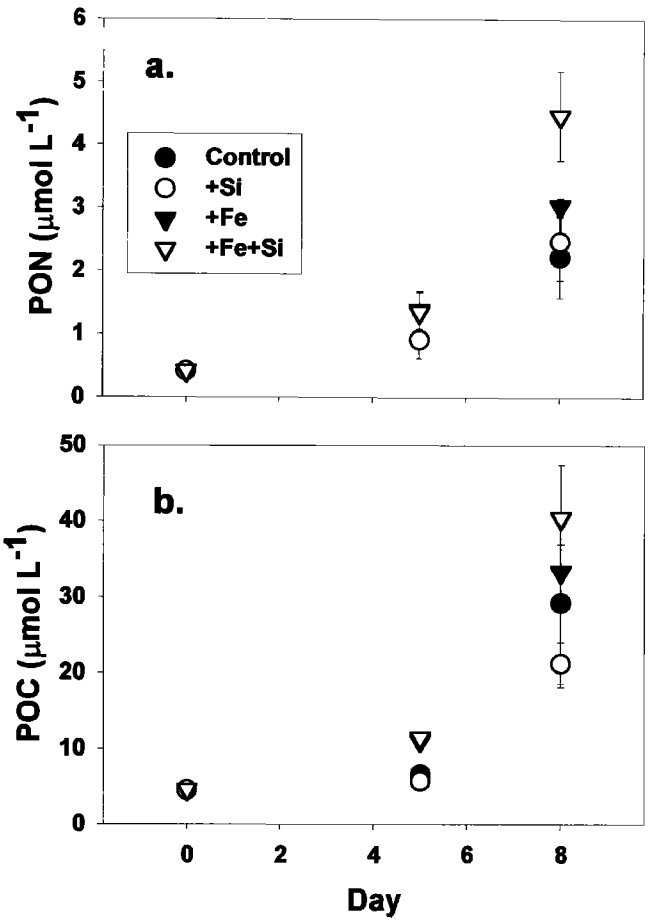

Figure 9. (a) PON and (b) POC concentrations in all four treatments over the course of the 2.4 L bottle incubations. Symbols and error bars are as in Figure 2.

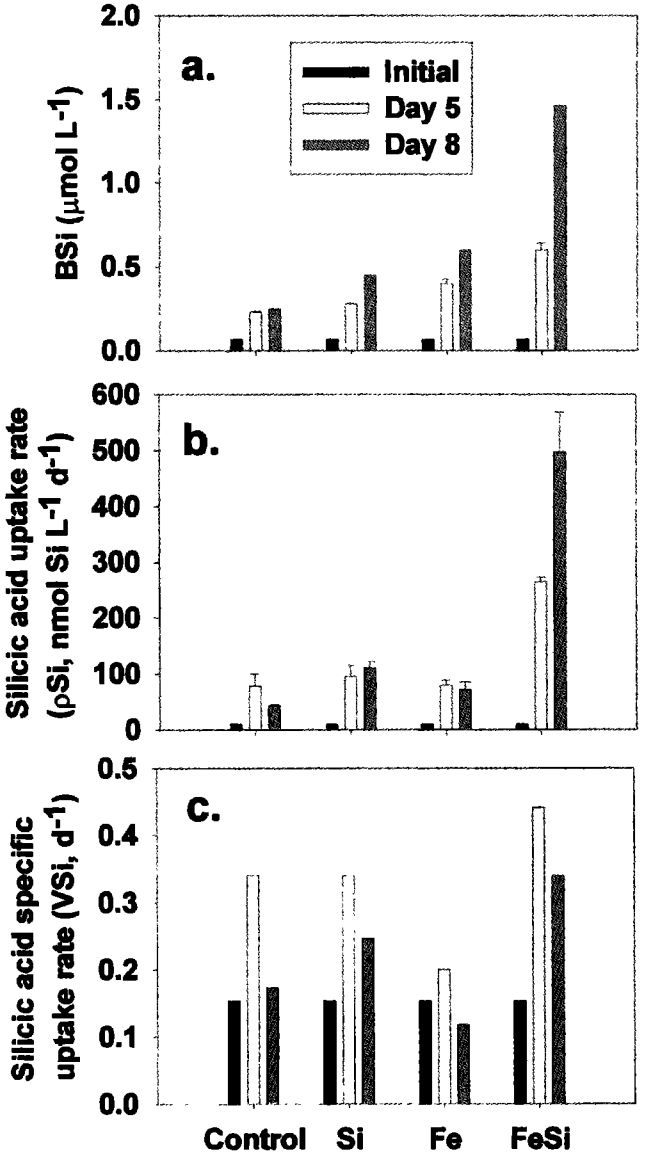

Figure 10. (a) BSi (nmol L^{-1}) concentrations, (b) ρSi (nmol Si L^{-1} d^{-1}), and (c) VSi (d^{-1}) in all four treatments over the 8 day incubations (initial values, black bars; day 5 values, white bars; and day 8 values, shaded bars). Values and error bars are the means and ranges of duplicate 2.4 L bottles.

2.4-5.8 times higher than in any of the other treatments. Absolute silicic acid uptake rates (ρSi, nmol Si L^{-1} day^{-1}) measured using ^{32}Si tracer showed a similar pattern, with significantly elevated rates ($p < 0.05$) measured in the +Fe+Si-treated bottles on days 5 and 8, compared with only modest increases observed in the other treatments relative to initial values (Figure 10b). Specific uptake rates of Si (VSi, d^{-1}) increased in the control, +Fe, and +Si treatments between the initial and day 5 timepoints (1.3 -2.2 times), but this increase was significantly greater (2.9 times) in the +Fe+Si samples (Figure 10c). VSi declined somewhat in all treatments between the day 5 and final timepoints, but was still 1.4 –2.9X higher in the +Fe+Si treatment than in the other three (Figure 10c).

As expected, given the low ambient silicic acid concentrations, very little BSi was produced in either the control (0.2 μmol L^{-1}) or +Fe (0.5 μmol L^{-1}) treatments. Measured BSi production was also very low in the bottles amended with ~9 μM silicic acid and no added Fe (0.4 μmol L^{-1} BSi). Much greater concentrations of BSi were produced (1.4 μmol L^{-1}) in bottles amended with both Si and Fe, although this production still represents only about 20% of the ~9.7 μM silicic acid present in these bottles after the initial Si additions. The production of BSi accounted for 120% (control), 93% (+Fe), ~70% (+Si), and ~73% (+Fe+Si) of the silicic acid drawdown measured in the incubation bottles (Figure 8c).

From the PON and BSi data we calculate the ratios of BSi:PON produced after 8 days in the 2.4 L incubation bottles as 0.10 (control), 0.20 (+Fe), ~0.18 (+Si), and ~0.34 (+Fe+Si). These ratios compare reasonably well with the Si:N consumption ratios calculated from the dissolved nutrient measurements, allowing for the large uncertainty in the dissolved Si drawdown in the +Si and +Fe+Si treatments (due to stock solution polymerization) and the inherent uncertainty in calculating differences from small changes in nutrient concentrations, as was the case in the control and +Fe treatments. These calculated BSi:PON production ratios confirm that Si:N uptake ratios are considerably less than 1 in our experiments and that these ratios apparently do not show the clear dependence on Fe availability that has been observed in other shipboard field studies.

At day 5 in the 24 L carboy incubations, total community (>0.2 μm) Fe uptake rates in the control treatments had not changed significantly from the initial levels ($p = 0.2$, Figure 11). The day 5 total community Fe uptake rates in the +Fe- and +Si-treated carboys were similar to each other and significantly higher (~3 times, $p < 0.02$) than in the control treatments. Iron uptake rates in the >0.2 μm size fraction in the +Fe+Si-treated carboys were greatly increased over initial values, and were significantly higher than day 5 rates in the control treatments (by ~4.7 times, $p = 0.03$) and in the +Fe and +Si treated carboys (by ~1.6 times, $p < 0.04$). These substantially higher Fe uptake rates in the +Fe+Si treated carboy were mostly due to increased Fe uptake rate in the 0.2- 5.0 μm size class, with also some contribution from increased uptake rate in the >5 μm size class (Figure 11).

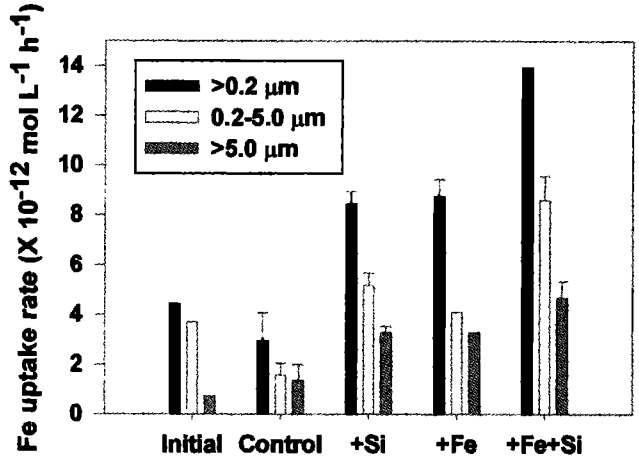

Figure 11. Biological Fe uptake rates (x10^{-12} mols Fe L^{-1} h^{-1}) calculated from ^{55}Fe incubations for three plankton size classes (>0.2 μm, black bars; 0.2-5 μm, white bars; and >5 μm, shaded bars) in the initial collected water and for all four treatments in the 24 L carboys on day 5 of the incubations. Values and error bars are the means and ranges of two ^{55}Fe incubations from each unreplicated carboy.

The molar Fe uptake rates in the +Fe+Si-treated carboys for the smaller (0.2- 5.0 μm) cells were significantly higher ($p < 0.05$) than those in either the control (by 5.5 times), +Si (by 1.7 times), or +Fe (by 2.1 times) treatment carboys. A similar trend was observed for the largest plankton size class (>5.0 μm). However, the day 5 uptake rates in the +Fe+Si-treated carboys were significantly higher than the control treatments ($p = 0.004$) but were not different from the rates in the +Si ($p = 0.5$) and +Fe ($p = 0.19$) treatments. Like the Si uptake rate results, the general picture is that the addition of Fe or Si alone increased biological Fe uptake rates relative to control treatments, but the addition of both Fe and Si resulted in the highest Fe uptake rates (Figure 11).

The results of HPLC pigment analyses, ^{14}C pigment labeling, and Fe uptake rate measurements from the 24 L carboy after 5 days incubation have already been presented (see Figures 6 and 11). In general, the biogeochemical and biological responses observed for a given treatment were remarkably similar on day 5 in the large (24 L) and small (2.4 L) containers (data not shown). Some minor differences in nutrient utilization and biological parameters were evident, but these did not exhibit a consistent trend with bottle size. This suggests that under these experimental conditions, enclosure size has only minor effects on the results of iron and nutrient addition bottle incubation experiments. This implies that measurements performed only for the large-volume incubations are probably applicable to the large- and small-volume incubation results.

4. Discussion

Our experiments suggest that Fe is the primary limiting nutrient in the subantarctic ecosystem in the late summer and autumn, but that lack of Si also impacts phytoplankton growth and community structure. This system is poised close to limitation by both Fe and Si. Addition of either alone resulted in increases in many biological and biogeochemical parameters, but addition of both Fe and Si together produced the most pronounced effects on the algal community.

Addition of Fe alone resulted in increases (relative to the controls) in total community chl *a*, photosynthetic efficiency (F_v/F_m), maximum carbon fixation rates (P_{max}), fucoxanthin concentrations, pennate diatom numbers, nitrate and phosphate drawdown, BSi concentrations, and silicic acid and iron uptake rates. Si added alone caused increases in eukaryotic picoplankton counted by flow cytometry, picoplankton chl *a* growth rates, BSi and silicic acid and iron uptake rates. It is apparent that additions of either Fe or Si alone allowed at least a limited amount of increased phytoplankton growth, although as discussed below, probably by somewhat different assemblages.

However, for many of these measured parameters both Fe and Si added together produced the largest effects. Those that were significantly higher at the 95% confidence level ($p = 0.05$) were P_{max} and α values, BSi, absolute iron uptake rates, and absolute and specific silicic acid uptake. At a lower confidence level of 90% ($p = 0.1$), >20 μm chl *a*, silicic acid drawdown, and PON and POC production were significantly elevated in the +Fe+Si treatments. Although they were not replicated (and so cannot be statistically compared), fucoxanthin concentrations were also much higher in +Fe+Si treatments than in either +Fe or +Si bottles.

The ^{32}Si and ^{55}Fe tracer incubations and the BSi measurements provide some of the strongest evidence for multiple limitation of the community by Fe and Si. BSi concentrations, ρSi, and VSi were significantly higher in the +Fe+Si treatment than in the other treatments (Figure 10). Fe uptake rates increased in both +Fe and +Si carboys compared to the control, but rates in the +Fe+Si carboy were much higher again (Figure 11). Thus uptake of both Fe and silicic acid responded more strongly to both Fe and Si added together than to either nutrient added alone. This suggests an additive effect of Fe and Si limitation on siliceous species such as diatoms. There is no evidence from the literature for a true colimitation between Fe and Si in which utilization of one nutrient is physiologically linked to the availability of the other (such as for Fe and nitrate). Nevertheless, limitation by both Fe and Si appears to be the case in low-Fe, low-Si subantarctic waters.

The HPLC pigment data show that levels of the haptophyte pigment 19-hex increased in all three addition treatments relative to the initial and day 5 control levels (Figure 6). Especially intriguing are the increases in this haptophyte marker after addition of Si alone since silicic acid availability is often assumed to be important only to diatoms. Despite the increase in absolute 19-hex concentration in the +Fe carboy, CHEMTAX analyses suggest that the relative abundance of type 4 haptophytes increased only slightly in both the control and +Fe bottles. Relative abundance increases were, however, much larger in the two treatments with added Si (Table 2). This taxonomic group includes silicoflagellates, as well as several groups that can have lightly silicified scales (such as the parmales). Silicic acid limitation of picoeukaryotes is also suggested by the higher chl *a* net growth rates of the 0.2-2.0 μm fraction in the +Si treatments relative to the controls (Tables 1 and 3). Flow cytometry counts lend additional support to the idea that siliceous flagellates may have responded to Si additions since increases in picoeukaryote numbers occurred only in the +Si and +Fe+Si treatments (Figure. 7c).

Siliceous haptophytes such as the silicoflagellates *Dictyocha speculum* and *Dictyocha fibula* were observed in microscopy samples collected at this station [*R. Greene and B. Griffiths*, unpublished data, 2001]. Our experimental results suggest that these haptophytes were limited by Si but probably were not severely Fe-limited. BSi concentrations did increase in the +Si bottles, although not dramatically (Figure 10a), consistent with the growth of lightly silicified picoeukaryotes. Despite light silicification this group might nevertheless be Si-limited, for instance, by high half-saturation constants for silicic acid uptake. These species, however, appear to have very low Fe requirements since their relative abundance was about the same regardless of Fe availability (Table 2). Our results suggest the need to consider little known nondiatom siliceous phytoplankton in future studies of the biogeochemical cycling of Fe and Si in the subantarctic region.

As in many previous Fe addition experiments [*Martin and Gordon*, 1990; *Martin et al.*, 1991; *Price et al.*, 1991; *Boyd et al.*, 1996; *Hutchins and Bruland*, 1998; *Bronk et al.*, in press], Fe addition (either with or without Si) significantly increased nitrate drawdown in our experiments (Figure 8a). We therefore conclude that Fe was the proximate control on nitrate utilization and new production by the phytoplankton community. Silicic acid drawdown was, however, much slower regardless of Fe availability (Figure 8c).

It is notable that Si:N (silicic acid to nitrate) net drawdown ratios in our incubations were very low (0.10-0.35) and were apparently unaffected by Fe availability. This conclusion is robustly supported by measurements of both dissolved nutrient drawdown and particulate BSi and PON production but is contrary to a number of previous observations in other low-Fe regimes [*Hutchins and Bruland*, 1998], including other parts of the Southern Ocean [*Takeda*, 1998; *Franck et al.*, 2000; *Boyd et al.*, 2000]. Low community Si:N ratios could be partly due to increases in small nanoplanktonic pennate diatoms as compared to larger diatoms. *Brzezinski* [1985] found a mean Si:N ratio of 1.20 (± 0.37) for >20 μm diatom taxa but a lower Si:N ratio of

0.85 (± 0.35) for <20 μm nanoplanktonic taxa. The pigment data also suggest that low Si:N utilization ratios were partly due to the growth of other, nondiatom species.

The fucoxanthin measurements and the visual cell counts demonstrated an unexpected amount of diatom growth in bottles amended with Fe alone, despite very low ambient silicic acid concentrations (0.66 μM). Apparently, the dominant small pennate diatoms were able to take advantage of increased Fe availability and deplete >83% (0.57 μM) of the ambient silicic acid, producing lightly silicified biomass. Normalization of Si used to diatom cells produced yields a value of ~0.06 pmol Si $cell^{-1}$, similar to the cell quota of many small pennates such as *Nitzschia* [*Brzezinski*, 1985]. What is more surprising is that this growth occurred by drawing silicic acid down almost to nanomolar levels. This substantial drawdown of the initially low silicic acid concentrations is remarkable in view of the high half-saturation constants (0.5-4.6 μM) that have been reported for Si uptake by diatoms from the Ross Sea [*Nelson and Tréguer*, 1992] and other oceanic areas such as the Sargasso *Sea* [*Nelson and Brzezinski*, 1990]. Our data suggest that addition of Fe to Si-depleted subantarctic waters can result in rapid growth of both very lightly silicified diatom species highly adapted to low-Si conditions and small nonsiliceous algae.

This interpretation of our results would explain why Fe additions did not result in the decreased Si:N uptake ratios that have been observed in other studies. Net drawdown ratios are likely to be quite different in high- and low-Si HNLC waters because of differences in both Si availability and community composition. In contrast to the picoplankton- and nanoplankton-dominated community found in Si-depleted subantarctic waters, large chain-forming diatoms and high silicic acid concentrations characterize the California upwelling region where this effect of Fe availability on Si:N ratios was first noted [*Hutchins and Bruland*, 1998; *Hutchins et al.*, 1998]. Larger populations of heavily silicified diatom species and higher dissolved Si concentrations may be present in the other areas where this Si:N ratio effect has been reported, including the equatorial Pacific, subarctic Pacific, and other parts of the Southern Ocean [*Takeda*, 1998; *Boyd et al.*, 2000]. Elevated Si:N uptake ratios under Fe-deficient conditions have also been reported from subantarctic experiments, but these were carried out closer to the Polar Front and earlier in the season when silicic acid was present at much higher concentrations (~5 μM) [*Franck et al.*, 2000].

We suggest that in the subantarctic, springtime high-Si conditions may allow the growth of large, robustly silicified diatoms (such as *Chaetoceros* and *Fragilariopsis*) that draw down silicic acid and nitrate at a high molar ratio (>2) under Fe stress. These species may be similar to the heavily silicified diatoms that typically dominate throughout the season in high-nitrate, high-silicic acid waters of the Antarctic Circumpolar Current [*Minas and Minas*, 1992] and the spring bloom in the Polar Frontal region [*Quéguiner et al.*, 1997]. As the growing season progresses in the Subantarctic, silicic acid becomes depleted, and these larger diatoms with relatively high requirements for Si and Fe may become unable to compete successfully. The community may then shift toward nonsiliceous picoplankton and nanoplankton and very small pennate diatoms capable of growing with very little silicic acid and Fe.

Our late summer experiments support the suggestion that there is a seasonal progression of limiting factors for phytoplankton growth in the subantarctic region [*Boyd et al.*, 1999; this issue]. A light-limited early spring community may evolve toward iron/light colimitation [*Sunda and Huntsman*, 1997; *Maldonado et al.*, 1999] as iron is depleted, then toward limitation mainly by iron as mixed layers begin to shallow in the summer [*Boyd et al.*, 1999; this issue]. We propose that iron limitation drives the depletion of silicic acid before other nutrients, and by late summer the community may be limited by both Fe and Si, as in our experiments. Community Si:N drawdown ratios may be quite low at this point and become decoupled from Fe availability. Relatively constant chl *a* concentrations in this region [*Banse*, 1996] may thus conceal important changes in community composition, as different limiting factors select for different algal taxa [*Boyd et al.*, 1999]. Fe and light colimitation [*Boyd et al.*, this issue] and Fe and Si interactions both appear to play a significant role in subantarctic biogeochemistry; possible interactions between Si and light limitation remain less well understood [*Nelson and Smith*, 1991; *Lippemeier et al.*, 1999].

Our results and the few data sets available from other work in this region suggest that multiple limiting factors (including Fe, Si, and light) are all important at times in the subantarctic Southern Ocean. Top down control by grazing was not investigated here but is undoubtedly also important [*Cullen*, 1991; *Banse*, 1996], especially for the small phytoplankton species that dominated in our experiments. Our experiments suggest that increases in aeolian Fe supplies during glacial periods (without simultaneously increased Si inputs) would have favored the growth of small, lightly silicified pennate diatoms and nonsiliceous picoplankton and nanoplankton. Such a community would likely export carbon less efficiently than the large diatom species that thrive when Fe and Si are both abundant and could account for the high organic carbon:opal ratios observed in glacial age seafloor sediments in the subantarctic region [*Kumar et al.*, 1995]. Increases in Si availability without concurrent Fe inputs, on the other hand, may shift community structure toward little studied species of nondiatom siliceous picoplankton.

Recent modeling work incorporating new evidence about Fe and Si interactions suggests that increased glacial era dust supplies could have led to widespread depletion of silicic acid throughout Southern Ocean surface waters [*Watson et al.*, 2000]. If so, conditions over much of the glacial Southern Ocean may have resembled those of the high-nitrate, low-silicic acid regime in the modern Subantarctic.

Interactions between Fe, Si, and light limitation such as those examined here and by *Boyd et al.* [this issue] would have had large consequences for primary productivity, phytoplankton community structure, and carbon export. The importance of the subantarctic Southern Ocean in present-day carbon cycling [*Metzl et al.*, 1999] and in glacial/interglacial climate oscillations [*Kumar et al.*, 1995] emphasizes the need for a better understanding of how these multiple limiting factors collectively influence phytoplankton growth throughout the region.

Acknowledgements. We thank the captain and crew of the RSV Aurora Australis, chief scientist T. Trull, our colleagues and technical staff involved in the SAZ project, and the Australian Antarctic Division for ship time and logistical support. Support was provided by NSF INT 9802132, OCE 9811062, University of Delaware startup funds (D.A.H.), INT 9724919 (G.R.D.), the Antarctic CRC, CSIRO Division of Marine Research, and ANARE.

References

Banse, K., Low seasonality of low concentrations of surface chlorophyll in the Subantarctic water ring: Underwater irradiance, iron, or grazing?, *Prog. Oceanogr.*, *37*, 241-249, 1996.

Berg G. M., P. M. Glibert, and C. C. Chen, Dimension effects of enclosures on ecological processes in pelagic systems, *Limnol. Oceanogr.*, *44*, 1331-1340, 1999.

Boyd, P. W., D. Muggli, D. Varela, R. H. Goldblatt, R. Chretien, K. J. Orians, and P.J. Harrison, In vitro iron enrichment experiments in the NE subarctic Pacific, *Mar. Ecol. Prog. Ser.*, *136*, 179-196. 1996.

Boyd P. W., J. LaRoche, M. Gall, R. Frew, and R. M. L. McKay, Role of iron, light, and silicate in controlling algal biomass in subantarctic waters SE of New Zealand, *J. Geophys. Res. O*, *104*, 13,395-13,408, 1999.

Boyd, P.W., A. C. Crossley, G. R. DiTullio, F. B. Griffiths, D. A.

Hutchins, B. Quéguiner, P. N. Sedwick, and T.W. Trull, Control of phytoplankton growth by iron supply and irradiance in the subantarctic Southern Ocean: Experimental results from the SAZ Project, *J. Geophys. Res.*, this issue.

Boyd, P. W., et al., A mesoscale phytoplankton bloom in the polar Southern Ocean stimulated by iron fertilization, *Nature*, *407*, 695-702, 2000.

Bronk, D. A. and B. B. Ward, Gross and net nitrogen uptake and DON release in the euphotic zone of Monterey Bay, California. *Limnol. Oceanogr.*, *44*, 573-585, 1999.

Bronk, D. A., B. R. Wheeler, III, W. P. Cochlan, K. H. Coale and S. E. Fitzwater. AESOPS: Effects of iron addition on nutrient depletion and nitrogen uptake rates in an offshore region of the Ross Sea, *Antarct. J. U.S.*, in press.

Brzezinski, M. A., The Si:C:N ratio of marine diatoms: Interspecific variability and the effect of some environmental variables, *J. Phycol.*, *21*, 347-357,1985.

Buma, A. G. J., H. J. W. de Baar, R. F. Nolting, and A. J. van Bennekom, Metal enrichment experiments in the Weddell-Scotia Seas: Effects of iron and manganese on various plankton communities. *Limnol. Oceanogr.*, *36*, 1865-1878, 1991.

Chang, F. H. and M. Gall, Phytoplankton assemblages and photosynthetic pigments during winter and spring in the subtropical convergence region near New Zealand. *N. Z. J. Mar. Freshwater Res.*, *32*, 515-530, 1998.

Crossley A. C, Shipboard flow cytometric analysis of protist population structure in the Southern Ocean, paper presented at VII Scientific Committee on Antarctic Research International Biological Symposium, Christchurch, N. Z. 1998.

Cullen, J. C, Hypotheses to explain high-nutrient conditions in the sea. *Limnol. Oceanogr.*, *36*, 1578-1599, 1991.

de Baar, H. J. W., A. G. J. Buma, R. F. Nolting, G. C. Cadee, G. Jacques, and P. J. Tréguer, On iron limitation of the Southern Ocean: Experimental observations in the Weddell and Scotia Seas. *Mar. Ecol. Prog. Ser.*, *65*, 105-122. 1990.

de Baar, H. J. W., J. T. M. de Jong, D. C. E. Bakker, B. M. Löscher, C. Veth, U. Bathmann, and V. Smetacek, Importance of iron for plankton blooms and carbon dioxide drawdown in the Southern Ocean, *Nature*, *373*, 412-415, 1995.

DiTullio, G. R., P. N. Sedwick , D. R. Jones, P. W. Boyd, A. C. Crossley, and D. A. Hutchins, Effects of iron, silicate, and light on dimethylsulfoniopropionate production in the Australian Subantarctic Zone, *J. Geophys. Res. Oceans*, this issue.

Dugdale, R. C. and F. P. Wilkerson, Silicate regulation of new production in the eastern equatorial Pacific, *Nature*, *391*, 270-273, 1998.

Dugdale, R. C., F. P. Wilkerson, and H. J. Minas, The role of a silicate pump in driving new production, *Deep-Sea Res. Part I*, *42*, 697-719, 1995.

Durand, M. D. and R. J. Olson, Contributions of phytoplankton light scattering and cell concentration changes to diel variations in beam attenuation in the equatorial Pacific from flow-cytometric measurements of pico-, ultra-, and nanoplankton, *Deep Sea Res. Part II*, *43*, 891-906, 1996.

Franck, V. M., M. A. Brzezinski, K. H. Coale, and D. M. Nelson, Iron and silicic acid availability regulate Si uptake north and south of the Polar Frontal Zone in the Pacific Sector of the Southern Ocean. *Deep-Sea Res. Part II*, *47*, 3315- 3338. 2000.

Geider, R. J., and J. LaRoche, The role of iron in phytoplankton photosynthesis, and the potential for iron-limitation of primary productivity in the sea, *Photosyn. Res.*, *39*, 275-301, 1994.

Greene, R. M., R. J. Geider, and P.G. Falkowski, Effect of iron limitation on photosynthesis in a marine diatom. *Limnol. Oceanogr.*, *36*, 1772-782, 1991.

Hofstraat, J. W., W. J. M. van Zeijl, M. E. J. de Vreeze, J. C. H. Peeters, L. Peperzak, F. Colijn and T. W. M. Rademaker, Phytoplankton monitoring by flow cytometry. *J. Plankton Research*, *16*, 1197-1224, 1994.

Hudson, R. J. M. and F. M. M. Morel, Distinguishing between extra- and intracellular iron in marine phytoplankton, *Limnol. Oceanogr.*, *34*, 1113-1120, 1989.

Hutchins, D. A. and K. W. Bruland, Iron-limited diatom growth and Si:N uptake ratios in a coastal upwelling regime, *Nature*, *393*, 561- 564, 1998.

Hutchins, D. A., G. R. DiTullio, Y. Zhang, and K. W. Bruland, An iron limitation mosaic in the California upwelling regime, *Limnol. Oceanogr.*, *43*, 1037-1054, 1998.

Hutchins, D. A., V. M. Franck, M. A. Brzezinski, and K. W. Bruland, Inducing phytoplankton iron limitation in iron-replete coastal waters with a strong chelating ligand, *Limnol. Oceanogr.*, *44*, 1009-1018, 1999.

Jeffrey, S. W., R. F. C. Mantoura, and S. W. Wright, *Phytoplankton Pigments in Oceanography*, *SCOR/UNESCO Monogr.*, Vol. 10. UNESCO Publ., Paris, 1997.

Kolber, Z. and P. G. Falkowski, Use of active fluorescence to estimate phytoplankton photosynthesis in situ, *Limnol. Oceanogr.*, *38*, 1646-1665, 1993.

Kumar, N., R. F. Anderson, R. A. Mortlock, P. N. Froelich, P. Kubik, B. Dittrich-Hannen, and M. Suter, Increased biological productivity and export production in the glacial Southern Ocean, *Nature*, *378*, 675-680, 1995.

Lippemeier, S., P. Hartig, and F. Colijn. Direct impact of silicate on the photosynthetic performance of the diatom *Thalassiosira weissflogii* assessed by on- and off-line PAM fluorescence measurements, *J. Plankton Res.*, *21*, 269-283, 1999.

Mackey, D. J., J. Parslow, H. W. Higgins, F. B. Griffiths, and J. E. O'Sullivan, Plankton productivity and biomass in the western equatorial Pacific: Biological and physical controls, *Deep Sea Res. Part II*, *42*, 499-533. 1995.

Maldonado, M., P. W. Boyd, N. M. Price, and P. J. Harrison, Co-limitation of phytoplankton by light and Fe during winter in the NE subarctic Pacific. *Deep Sea Res. Part II*, *46*, 2475-2486, 1999.

Martin, J. H., and R. M. Gordon, Iron deficiency limits phytoplankton growth in Antarctic water, *Global Biogeochem.Cycles*, *4*, 5-12, 1990.

Martin, J. H., R. M. Gordon, and S. E. Fitzwater, The case for iron. *Limnol. Oceanogr.*, *36*, 1793-1802, 1991.

Measures, C. I., J. Yuan,, and J. A. Resing, Determination of iron in seawater by flow injection-analysis using in-line preconcentration and spectrophotometric detection, *Mar. Chem.*, *50*, 3-12, 1995.

Metzl, N., B. Tilbrook, and A. Poisson, The annual fCO_2 cycle and air-sea CO_2 flux in the sub-Antarctic Ocean, *Tellus* Ser. B, *51*, 849-861, 1999.

Minas, H. J. and M. Minas, Net community production in "High Nutrient-Low Chlorophyll" waters of the tropical and Antarctic Oceans: Grazing versus iron hypothesis, *Oceanol. Acta*, *15*, 145-162, 1992.

Nelson, D. M. and M. A. Brzezinski, Kinetics of silicic acid uptake by natural diatom assemblages in two Gulf Stream warm-core rings, *Mar. Ecol. Prog. Ser.*, *62*, 283-292, 1990.

Nelson, D. M. and W. O. Smith, Sverdrup revisited: Critical depths, maximum chlorophyll levels, and the control of Southern Ocean productivity by the irradiance-mixing regime, *Limnol. Oceanogr.*, *36*, 1650-1661, 1991.

Nelson, D. M. and P. Tréguer, Role of silicon as a limiting nutrient to Antarctic diatoms: Evidence from kinetic studies in the Ross Sea ice-edge zone, *Mar Ecol. Prog. Ser.*, *80*, 255-264, 1992.

Olson, R. J., H. M. Sosik, A. M. Chekalyuk, and A. Shalapyonok, Effects of iron enrichment on phytoplankton in the Southern Ocean during late summer: Active fluorescence and flow cytometric analyses, *Deep Sea Res Part II*, *47*, 3181- 3200, 2000.

Olson, R. J., E. R. Zettler and M. D. DuRand, Phytoplankton analysis using flow cytometry, in Handbook of Methods in Aquatic Microbial Ecology, edited by P. F. Kemp, pp. 175-186, A. F., Lewis, New York, 1993.

Price, N. M., L. F. Andersen, and F. M. M. Morel, Iron and nitrogen nutrition of equatorial Pacific plankton, *Deep Sea Res.Part A* , *38*, 1361-1378, 1991.

Quéguiner, B., P. Tréguer, I. Peeken, and R. Scharek, Biogeochemical dynamics and the silicon cycle in the Atlantic sector of the Southern Ocean during austral spring 1992, *Deep Sea Res. Part II*, *44*, 69-89, 1997.

Quéguiner, B, Biogenic silica production in the Australian sector of the Subantarctic Zone of the Southern Ocean in late summer 1998, *J. Geophys. Res. Oceans*, This issue.

Rintoul S. R. and T. W. Trull, Seasonal evolution of the mixed layer in the Subantarctic Zone south of Australia, *J. Geophys. Res.*, this issue.

Schmidt, M. A. and D. A. Hutchins, Size-fractionated biological iron and carbon uptake along a coastal to offshore transect in the NE Pacific. *Deep Sea Res. Part II*, *46*, 2487-2503, 1999.

Sedwick, P. N., G. R. DiTullio, D. A. Hutchins, P. W. Boyd, F. B. Griffiths, A. C. Crossley, T. W. Trull, and B. Quéguiner, Limitation of algal growth by iron deficiency in the Australian Subantarctic region. *Geophys. Res. Lett.*, *26*, 2865-2868, 1999.

Sedwick, P. N., P. R. Edwards, D. J. Mackey, F. B. Griffiths, and J. S. Parslow, Iron and manganese in surface waters of the Australian subantarctic region, *Deep Sea Res. Part I*, *44*, 1239-1253, 1997.

Sunda, W. G. and S. A. Huntsman, Interrelated influence of iron, light, and cell size on marine phytoplankton growth, *Nature*, *390*, 389-392, 1997.

Takeda, S. Influence of iron availability on nutrient consumption ratio of diatoms in oceanic water, *Nature*, *393*, 774-777, 1998.

Trull, T., S. Bray, S. Manganini, R. Francois and S. Honjo, Moored sediment trap measurements of carbon export in the Subantarctic and

Polar Frontal Zones of the Southern Ocean, south of Australia, *J. Geophys. Res.*, this issue.

Watson, A. J., D. C. E. Bakker, A. J. Ridgewell, P. W. Boyd, and C. S. Law, Effect of iron supply on Southern Ocean CO_2 uptake and implications for glacial atmospheric CO_2 *Nature*, *407*, 730-733, 2000.

Wright, S. W., D. P. Thomas, H. J. Marchant, H. W. Higgins, M. D. Mackey, and D. J. Mackey, Analysis of phytoplankton of the Australian sector of the Southern Ocean: Comparisons of microscopy and size frequency data with interpretations of pigment HPLC data using the "CHEMTAX" matrix factorization program, *Mar. Ecol. Prog. Ser.*, *144*, 285-298, 1996.

Wright, S. W., R. van den Enden, R. Waters, P. Strutton, A. C. Crossley, P. Scott, F. B. Griffiths, P. Bonham, and H. J. Marchant, Protist population structure and dynamics in the Southern Ocean during Jan - Mar 1996, paper presented at VII Scientific Committee on Antarctic Research International Biological Symposium, Christchurch, N.Z. 1998.

(Received March 3, 2000; revised May 14, 2001;
accepted May 14, 2001.)